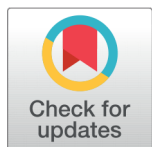


RESEARCH ARTICLE

 OPEN ACCESS

Received: 01-04-2022

Accepted: 25-05-2022

Published: 06-08-2022

Citation: Jebaraj PG, Sivashankar V (2022) Investigations on the Growth and Characterization of L-Leucine Doped Rubidium Sulfate Nonlinear Optical Single Crystal. Indian Journal of Science and Technology 15(30): 1473-1483. <https://doi.org/10.17485/IJST/V15I30.736>

* **Corresponding author.**

gershomjeba@gmail.com

Funding: None

Competing Interests: None

Copyright: © 2022 Jebaraj & Sivashankar. This is an open access article distributed under the terms of the [Creative Commons Attribution License](#), which permits unrestricted use, distribution, and reproduction in any medium, provided the original author and source are credited.

Published By Indian Society for Education and Environment ([iSee](#))

ISSN

Print: 0974-6846

Electronic: 0974-5645

Investigations on the Growth and Characterization of L-Leucine Doped Rubidium Sulfate Nonlinear Optical Single Crystal

P Gershom Jebaraj^{1*}, V Sivashankar²

¹ Research Scholar, Reg.No. 18231282131041, Department of Physics, St. Xavier's College (Autonomous), Palayamkottai, Affiliated to Manonmaniam Sundaranar University, Tirunelveli, India

² Assistant Professor, Department of Physics, St.Xavier's College (Autonomous), Palayamkottai, Affiliated to Manonmaniam Sundaranar University, Tirunelveli, India

Abstract

Objectives: To grow crystal of inorganic material Rubidium sulfate by doping with an organic material L-leucine. **Methods:** Crystal has been grown by solution method. Crystallographic studies were done. Mechanical studies were carried out to find the mechanical strength and other parameters. Dielectric studies of L-leucine doped rubidium sulfate crystals were carried out to evaluate dielectric constant, dielectric loss and activation energy. UV-visible-NIR spectral studies were done in the wavelength range 200-1100 nm. Second order Non Linear Optical (NLO) studies of the grown crystal of LLRS were carried out by Kurtz-Perry technique. **Findings:** The grown LLRS crystal is observed to be crystallizing in orthorhombic structure by single crystal XRD studies. The optical band gap of LLRS crystal was found to be slightly more than that of undoped rubidium sulphate crystal. The SHG efficiency of LLRS crystal is observed to be 0.61 times that of the reference KDP sample. Dielectric parameters are found to decrease with increase in frequency. Dielectric constant and dielectric loss factor increase when the temperature of the samples increases. AC conductivity increases with increase of temperature. Activation energy is increasing when the frequency increases. The band gap value is found to be 4.43 eV for undoped rubidium sulfate crystal. For L-leucine doped rubidium sulfate (LLRS) crystal, the optical band gap is 4.48 eV. From the Microhardness test, it is observed that the hardness increases with increase of the applied load for both the samples and this is due to reverse indentation size effect. **Novelty:** In this study, as a novel work, a very first attempt has been made to combine an organic material L-leucine with an inorganic crystal viz. rubidium sulfate to alter its physical and chemical properties.

Keywords: Inorganic Single Crystal; Crystal Structure; Mechanical Properties; Dielectric properties; Optical Properties; Spectral Properties

1 Introduction

Amino acids of possessing specific properties such as molecular chirality, which secures acentric crystallographic structures, and absence of strongly conjugated bonds lead to high transparency ranges in the visible and UV spectral regions. They are coming under the coformers.⁽¹⁾ An inorganic class of materials exhibits good second order nonlinear optical characteristics and attract the attention of scientists throughout the world for their ability to organize themselves in the form of single crystal with wide transparency window. These materials are also possessing better advantages compared to organic counterparts⁽²⁾. The designing of photonic devices need optically responsive material and thus the quest for discovering new optical material is always an upcoming field for scientists and researchers throughout the globe⁽³⁾. The inherent nature of amino acid holds a driving force that can widely alter the properties of the host material⁽⁴⁾. As far as crystal growth from slow solution evaporation technique is concerned, the use of an additive is the most convenient and impactful approach to optimize the intrinsic and extrinsic properties of a crystal⁽⁵⁾. L-leucine is an essential amino acid and it has been grown and studied by Soma Adhikari et al.⁽⁶⁾. Najjar et al. have grown and studied rubidium sulfate complex crystal like lithium rubidium sulphate by slow evaporation technique. Single crystal X-ray diffraction analysis shows that the crystal belongs to a monoclinic system and some physical parameters like plasma energy, Penn gap, Fermi energy and electronic polarizability have been evaluated for the grown crystal⁽⁷⁾. In this study, as a novel work, a very first attempt has been made to combine an organic material L-leucine with an inorganic crystal viz. rubidium sulfate to alter its physical and chemical properties. With the addition, most of the properties were altered. The band gap was evaluated by the extrapolation of the linear part to the energy axis and its value is found to be 4.43 eV for undoped rubidium sulfate crystal and for L-leucine doped rubidium sulfate (LLRS) crystal, the optical band gap is 4.48 eV.

2 Methodology

High purity AR grade L-leucine was purchased commercially from Merck India. The Chemical Abstracts Service (CAS) number of L-leucine is 61-90-5. Rubidium sulfate was purchased commercially from sigma Aldrich. The purity is 99.8%. CAS number is 7488-54-2. Initially, saturated solution was prepared using rubidium sulfate and double distilled water and 1 mole% of L-leucine was added into the solution. The solution was stirred for about 4 hours using a hot plate magnetic stirrer and during the stirring the hotplate was switched on and it was maintained at temperature of 50°C. Then, the solution was cooled to room temperature and it was filtered using the good quality Whatmann filter paper. The slightly hot solution was kept in broad glass vessel and after 4 or 5 days, transparent seed crystals were obtained. Again the saturated solution of the reactants were prepared in a beaker and some good quality seed crystals were placed at the bottom of the beaker covered with a perforated sheet. Due to slow evaporation, the seed crystals were turned into big-sized crystals after the growth period of 30 days.

3 Results and discussion

3.1 Finding the crystal structure and lattice parameters

X-ray diffraction (XRD) method is used to find the lattice parameters and hence the crystal structure. There are two XRD methods namely powder XRD method and single crystal XRD method to find the crystal structure. Since the sample is a single crystal, single crystal XRD method was adopted to solve the crystal structure. Single crystal X-ray diffractometer collects crystallographic data required for structure determination. The grown LLRS crystal was subjected to single crystal X-ray diffraction study at room temperature with MoK α radiation ($\lambda = 0.71073 \text{ \AA}$) using Bruker-Nonius MACH3/CAD4 diffractometer and the structural data were obtained. The obtained single crystal XRD data for L-leucine doped rubidium sulfate (LLRS) crystal are presented in Table 1. From the obtained data, it is observed that LLRS crystal belongs to orthorhombic system. For comparison purpose, the lattice parameters of undoped rubidium sulfate crystal were also found and the data are provided in the same table. When we compare the data, the crystal structure of undoped and L-leucine doped rubidium sulfate crystals are the same and due to doping of L-leucine into the lattice of rubidium sulfate crystal, the crystal structure does not altered.

Table 1. XRD data of undoped rubidium sulfate and L-leucine doped rubidium Sulfate (LLRS) crystals

Sample	Parameters (Å)			Unit cell volume (Å ³)	α°	β°	γ°
	a	b	c				
Undoped rubidium sulfate crystal	7.808 (3) Å	5.959 (4) Å	10.392 (2) Å	483.52(3)	90	90	90
LLRS crystal	7.791 (2) Å	5.963 (5) Å	10.411 (4) Å	484.05(2)	90	90	90

3.2 Dielectric properties

Dielectric properties like dielectric constant and dielectric loss of LLRS crystal were measured by using an LCR meter at different frequencies and temperatures. These properties are correlated with electro-optic property. Rubidium is applied in the field of optical fibre telecommunication networks, photomultiplier tubes, biomedical research and solar panels are used as an insulator in the ceramic sector owing to its large dielectric constant⁽⁸⁾. The polished single crystal of LLRS was electroded on either side with graphite coating to make it behave like a parallel plate capacitor. The dielectric constant of the crystal was calculated using the relation $\epsilon_r = C/C_o$, where C is the capacitance of the capacitor in the presence of the crystal and C_o is the capacitance in air. The measurement of dielectric constant and loss as a function of frequency and temperature gives the ideas of electrical processes that are taking place in materials. The variations of dielectric constant and dielectric loss for undoped and L-leucine doped rubidium sulfate crystal with frequency at room temperature are shown in the Figures 1 and 2. The ϵ_r is consequence of electronic, ionic, dipolar and space charge polarization. As thermal energy is provided to the crystal its ϵ_r is largely contributed by activeness of space charge polarization and so it is witnessed that the ϵ_r of studied crystals significantly enlargement with increase in temperature⁽⁹⁾. The lower dielectric constant indicates that the material offers less power consumption, low RC delay and minimum crosstalk which are most desirable factors for designing various photonic devices^(10,11). The variations of dielectric constant and dielectric loss for L-leucine doped rubidium sulfate crystal at different frequencies and temperatures are depicted in the Figures 3 and 4. It is noticed that the dielectric constant and dielectric loss factor increase when the temperature of the samples increases.

The AC conductivity (σ_{ac}) as calculated using the relation $\sigma_{ac} = 2\pi f \epsilon_o \epsilon_r \tan \delta$, where f is the frequency of the AC supply, ϵ_o is the permittivity of free space or vacuum (8.852×10^{-12} F/m), ϵ_r is the relative permittivity or dielectric constant and $\tan \delta$ is the dissipation factor or dielectric loss. The calculated values of AC conductivity for LLRS crystal are given in the Figures 5 and 6. From the results, it is observed that AC conductivity increases with increase of temperature of the sample and this is due to excitation of charged carriers from valence band to conduction band when the temperature is increased. For many substances, as the temperature increases more and more defects are produced which, in turn, increase the conductivity. The defect concentration will increase exponentially with temperature and consequently the electrical conduction also increases. Also the added L-leucine into the lattice of LLRS crystal will act as the defect and conductivity increases with temperature⁽¹²⁾.

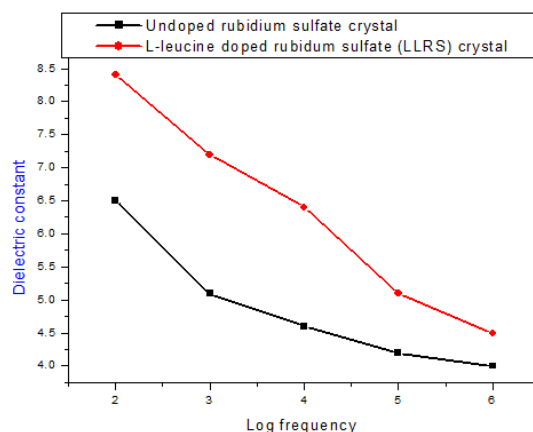


Fig 1. Variation of dielectric constant for undoped and L-leucine doped rubidium sulfate crystal with frequency at room temperature (30°C)

AC conductivity (σ_{ac}) of the sample obeys the Arrhenius relation and the Arrhenius relation for a dielectric or insulating material is given by $\sigma_{ac} = \sigma_o \exp(-E/kT)$ where σ_o is the pre-exponential factor, E is the activation energy for the AC conduction process and k is the Boltzmann's constant. By taking natural logarithm on both sides of the Arrhenius relation, the obtained expression is $\ln(\sigma_{ac}) = \ln(\sigma_o) - E/kT$ and this is an equation of the straight line. By finding slope value, the value of activation energy (E) can be obtained. For finding the values of slopes at different frequencies, the plots of $\ln(\sigma_{ac})$ versus $1000/T$ were drawn and they are provided in the Figures 7, 8, 9 and 10. Using the relation $E = \text{slope} \times k$, the values of activation energy at different frequencies like 10^2 Hz, 10^3 Hz, 10^4 Hz and 10^6 Hz are determined and the obtained values of activation energy for L-leucine doped rubidium sulfate (LLRS) crystal are given the Table 2. From the results, it is seen that activation energy is increasing when the frequency increases.

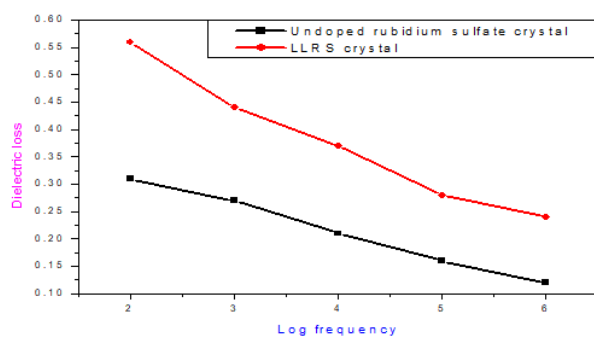


Fig 2. Variation of dielectric loss for undoped and L-leucine doped rubidium sulfate crystal with frequency at room temperature (30°C)

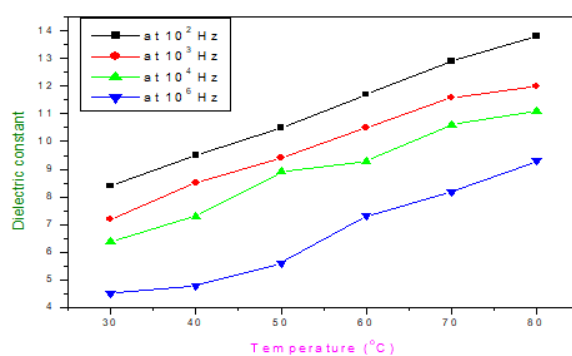


Fig 3. Variation of dielectric constant for L-leucine doped rubidium sulfate crystal at different frequencies and temperatures

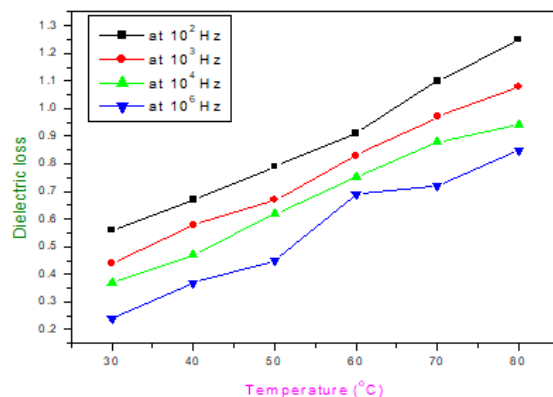


Fig 4. Variation of dielectric loss for L-leucine doped rubidium sulfate crystal at different frequencies and temperatures

Table 2. Values of activation energy for LLRS crystal at various frequencies

Frequency (Hz)	Activation energy (eV)
102	0.242
103	0.261
104	0.283
106	0.377

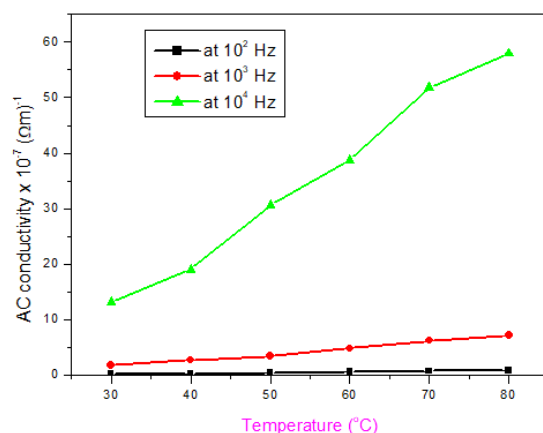


Fig 5. Temperature dependence AC conductivity for L-leucine doped rubidium sulfate crystal at 10^2 Hz, 10^3 Hz and 10^4 Hz.

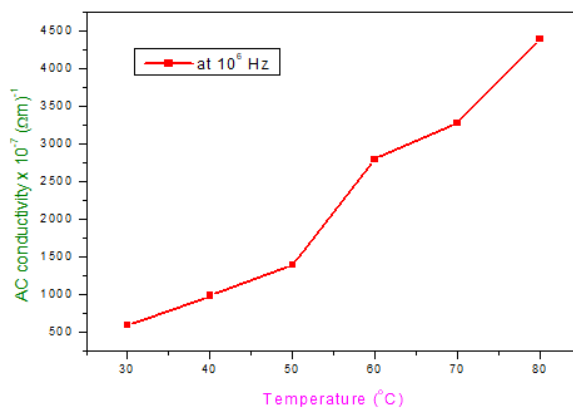


Fig 6. Temperature dependence AC conductivity for L-leucine doped rubidium sulfate crystal at 10^6 Hz

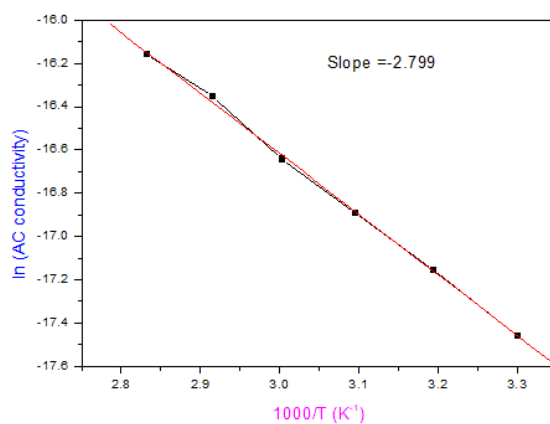


Fig 7. Plot of $\ln(\text{AC conductivity})$ versus $1000/T$ for LLRS crystal at Frequency of 10^2 Hz

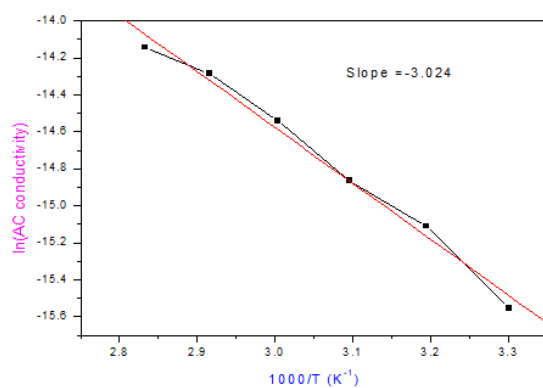


Fig 8. Plot of ln (AC conductivity) versus 1000/T for LLRS crystal at Frequency of 10³ Hz

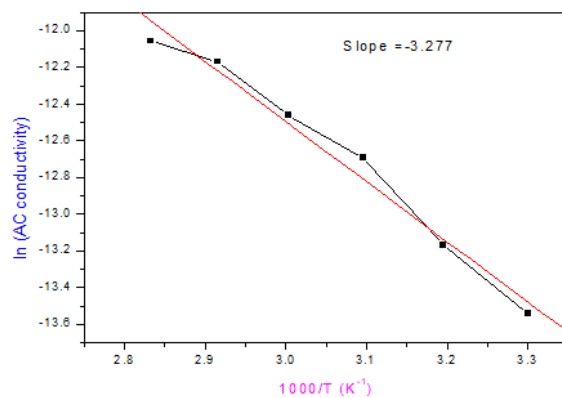


Fig 9. Plot of ln (AC conductivity) versus 1000/T for LLRS crystal at Frequency of 10⁴ Hz

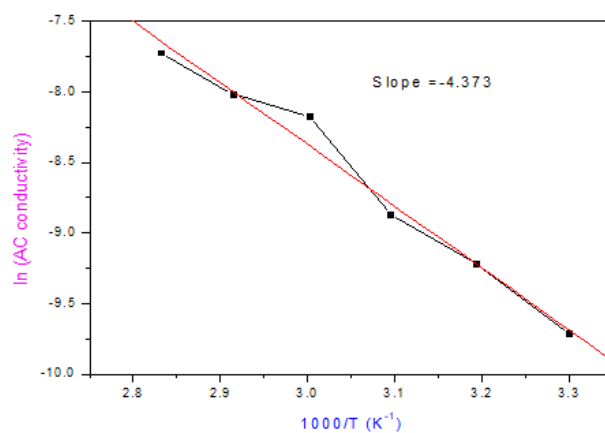


Fig 10. Plot of ln (AC conductivity) versus 1000/T for LLRS crystal at Frequency of 10⁶ Hz

3.3 Measurement of SHG

Nonlinear optics is a new process in which light of one wavelength is converted to light of another wavelength and the creation of light of new wavelength is due to the electrons in nonlinear crystals. At high fields, polarization becomes independent of the field and the susceptibility becomes field dependent. Measurement of SHG for undoped and L-leucine doped rubidium sulphate (LLRS) crystals was carried out by Kurtz and Perry test⁽¹³⁾. The powdered sample was illuminated using the Nd: YAG laser using the first harmonics output of 1064 nm with pulse width of 8ns and repetition rate 10 Hz. From the study, it is confirmed that there is no green laser light emission from undoped rubidium sulfate crystal. But it is observed that green laser light emitted from LLRS crystal when it was irradiated with Nd: YAG laser. Here potassium dihydrogen phosphate (KDP) crystal was used as the reference material. The result indicates that the relative SHG efficiency of LLRS crystal is 0.61 times that of KDP. Hence LLRS crystal is better than undoped rubidium sulfate crystal as far as the NLO applications are concerned.

3.4 UV-visible spectral studies

In UV-visible spectroscopy, the electrons involved are usually the valence or the bonding electrons, which can be excited by absorption of UV or visible or near IR radiation. The quantity of absorption depends on the wavelength of the radiation and the structure of the compound. The radiation absorption is due to the subtraction of energy from the radiation beam when electrons in orbitals of lower energy are excited into orbitals of higher energy. After the sample absorbs a portion of the incident radiation, the remainder is transmitted on to a detector where it is changed into an electrical signal and displayed after amplification. The transmission spectrum shows what percentage of the incoming light that actually makes it through the sample. UV-visible spectrum gives information about the structure of the molecule, because the absorption of UV and visible light involves promotion of the electron in the σ and π orbital from the ground state to higher states. The UV-visible spectrum of LLRS crystal was recorded using Perkin Elmer Lambda 35 UV-Visible spectrophotometer in the wave length range 200-1100 nm and the spectrum is shown in Figure 11. For comparison purpose, the spectrum of undoped rubidium sulfate crystal has also been recorded and it is shown in the same Figure 11.

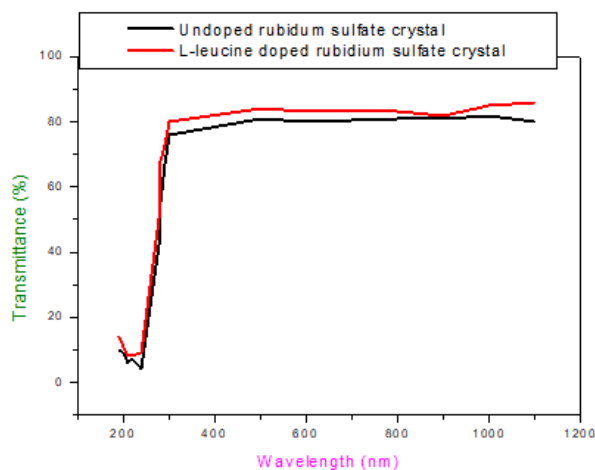


Fig 11. UV-visible spectra of undoped and L-leucine doped Rubidium sulfate crystals

From the UV-visible transmission spectra, it is observed that both undoped and L-leucine doped rubidium sulfate crystals have high transmittance in the visible region and hence they have a wide optical transmission window. The UV cut-off wavelength values are observed to be at 280 nm and 278 nm respectively for undoped and L-leucine doped rubidium sulfate crystals. This observation ascertains the fact that the crystals can be used for laser applications.

The measured transmittance (T) was used to calculate the absorption coefficient (α) using the formula:

$$\alpha = \frac{2.303}{t} \log \left(\frac{1}{T} \right)$$

Where 't' is the thickness of the sample.

The plots of absorption coefficient versus wavelength for both the samples are shown in the Figure 12. The result indicates that the absorption coefficient of the samples are low in the visible region. The dependence of optical absorption coefficient on photon energy is used to study the band structure and the type of transition electrons. The optical band gap was evaluated from

the transmission spectra and the optical absorption coefficient α near the absorption edge is given by

$$\alpha = \frac{A(h\nu - E_g)^n}{h\nu}$$

Where E_g is the optical band gap of the crystal and A is a constant. For a direct transition $n = 1/2$ depending on whether the transition is allowed in quantum mechanical sense. The plots of $(\alpha h\nu)^2$ versus $h\nu$ (Tauc's plot) are shown in Figure 13. The band gap was evaluated by the extrapolation of the linear part to the energy axis and its value is found to be 4.43 eV for undoped rubidium sulfate crystal and for L-leucine doped rubidium sulfate (LLRS) crystal, the optical band gap is 4.48 eV. Hence, the band gap of LLRS crystal is slightly more than that of undoped rubidium sulfate crystal. The extinction coefficient (K) can be obtained from the following relation:

$$K = \frac{\lambda\alpha}{4\pi}$$

The extinction coefficient as a function of wavelength for both the samples are presented in the Figure 14. It is observed that extinction coefficient of the samples is high at cut-off wavelength and it is found to be increasing with increase of wavelength in the visible region⁽¹⁴⁾.

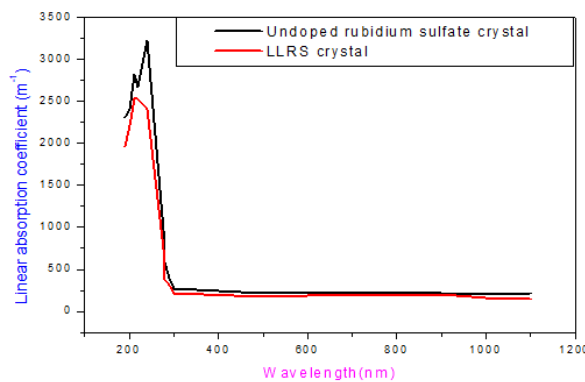


Fig 12. Plots of absorption coefficient versus wavelength for undoped and L-leucine doped rubidium sulfate (LLRS) crystals

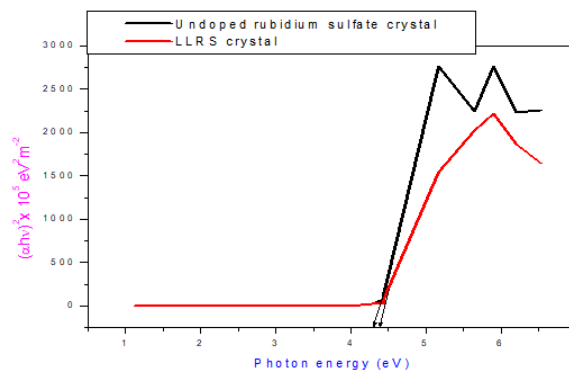


Fig 13. Tauc's plots for undoped and L-leucine doped rubidium sulfate crystals

3.5 Micro hardness, stiffness constant and yield strength

The micro hardness of the sample was measured by using the Vickers micro hardness tester. In this experiment, a pyramidal indenter was used. By applying loads, the average diagonal indentation was measured and using these values, the micro hardness number was determined. Using the values of average diagonal indentation, the micro hardness number (H_v) of the undoped and L-leucine doped rubidium sulfate (LLRS) crystals was calculated using the formula $H_v = 1.8544 \times P / d^2$ where, P is the

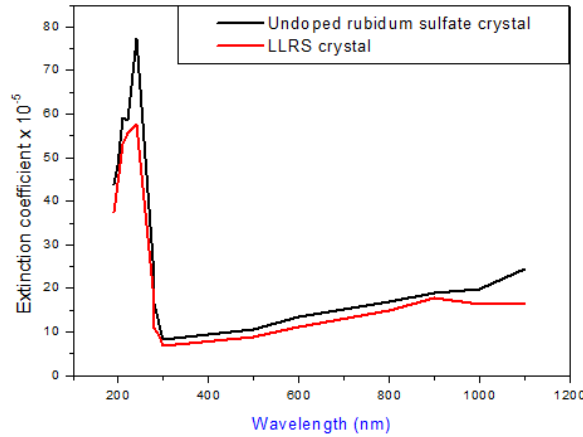


Fig 14. Variation of extinction coefficient with wavelength for undoped and L-leucine

applied load and d is the diagonal length of indentation. The plots of micro hardness versus applied load for both the crystals are shown in the Figure 15. It is observed that the hardness increases with increase of the applied load for both the samples and this is due to reverse indentation size effect. Yield strength is defined as the maximum stress that can be developed in a material without causing plastic deformation and it is also called as the yield stress. It is related to the yield point and it is the point on the stress-strain curve that indicates the limit of elastic behavior and the beginning of plastic behavior. Prior to the yield point the material will deform elastically and will return to its original shape when the applied stress is removed. Once the yield point is passed, some fraction of the deformation will be permanent and non-reversible. Yield strength depends on micro hardness (H_v) and the relation used for calculating the yield strength is $(\sigma_y) = (H_v/3)$. Another mechanical property viz., stiffness constant (C_{11}) is determined using the relation $C_{11} = H_v^{7/4}$ where H_v is the micro hardness of the sample. The calculated values of yield strength for both the samples are provided in the Table 3. From the data, it is observed that both yield strength and stiffness constant of the samples are high these values are increasing with increase of applied load. The values of stiffness constant of the samples are given in the Table 4. Stiffness constant of the samples are also increases as the load increases. Since hardness, yield strength and stiffness constant of undoped and L-leucine doped rubidium sulfate (LLRS) crystals are high, these crystals can be used for NLO device fabrication (15,16).

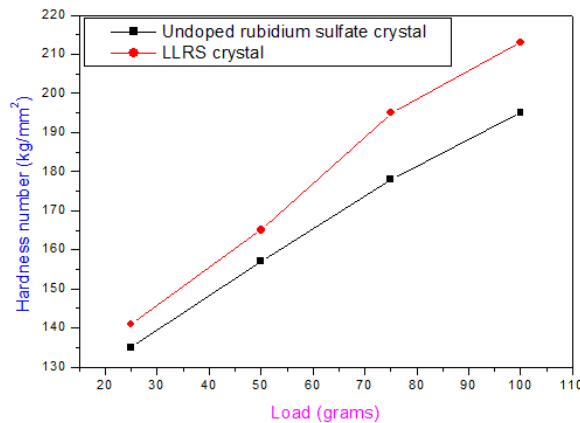


Fig 15. Plots of micro hardness number versus applied load for undoped and L-leucine doped rubidium sulfate (LLRS) crystals

Table 3. Values of yield strength for undoped and L-leucine doped rubidium sulfate (LLRS) crystals

Load (gram)	Yield strength (Mega pascal)	
	Undoped rubidium sulphate crystal	LLRS crystal
25	441.01	460.62
50	512.86	539.42
76	581.46	637.11
100	637.10	695.83

Table 4. Values of stiffness constant for undoped and L-leucine doped rubidium sulfate crystals

Load (gram)	Stiffness constant (pascal)	
	Undoped rubidium sulphate crystal	LLRS crystal
25	9.17761E+15	9.90328E+15
50	1.19528E+16	1.30389E+16
76	1.48895E+16	1.74665E+16
100	1.74665E+16	2.0385E+16

4 Conclusions

L-leucine has been added into the lattice of rubidium sulphate crystal to alter its properties. Aqueous solution growth method was adopted to grow the single crystals of L-leucine doped rubidium sulphate (LLRS). From the obtained crystallographic data, it is observed that LLRS crystal belongs to orthorhombic system. It is also found that doping of L-leucine into the lattice of rubidium sulfate crystal, the crystal structure does not altered. From the dielectric studies it is evident that, the dielectric parameters are found to decrease with increase in frequency. It is noticed that the dielectric constant and dielectric loss factor increase when the temperature of the samples increases. From the results, it is observed that AC conductivity increases with increase of temperature of the sample and this is due to excitation of charged carriers from valence band to conduction band when the temperature is increased. From the AC Conductivity results, it is seen that activation energy is increasing when the frequency increases. The second harmonic generation result indicates that the relative SHG efficiency of LLRS crystal is 0.61 times that of KDP. From the UV-visible transmission spectra, it is observed that both undoped and L-leucine doped rubidium sulfate crystals have high transmittance in the visible region and hence they have a wide optical transmission window. The band gap was evaluated by the extrapolation of the linear part to the energy axis and its value is found to be 4.43 eV for undoped rubidium sulfate crystal and for L-leucine doped rubidium sulfate (LLRS) crystal, the optical band gap is 4.48 eV. From the Microhardness test, it is observed that the hardness increases with increase of the applied load for both the samples and this is due to reverse indentation size effect.

5 Acknowledgement

The authors are thankful to the staff members of St. Joseph's college, Trichy, Cochin University, Cochin and Crescent Engineering College, Chennai for the research support to carry out this investigation.

References

- 1) Medvedev AG, Churakov AV, Prikhodchenko PV, Lev O, Vener MV. Crystalline Peroxosolvates: Nature of the Coformer, Hydrogen-Bonded Networks and Clusters, Intermolecular Interactions. *Molecules*. 2021;26(1):26–26. Available from: <https://dx.doi.org/10.3390/molecules26010026>.
- 2) Ramteke SP, Azhar SM, Muley GG, Baig MI, Alshehri AM, Somaily HH, et al. Growth and optimization of optical traits of copper sulphate crystal exploiting L-ascorbic acid for photonic device applications. *Chinese Journal of Physics*. 2021;71:168–174. Available from: <https://doi.org/10.1016/j.cjph.2020.04.006>.
- 3) Baig MI, Anis M, Shirsat MD, Hussaini SS, Algarni H. Comparative analysis of pristine and Cd²⁺ influenced potassium acid phthalate single crystal for photonic device applications. *Optik*. 2020;203:163903–163903. Available from: <https://doi.org/10.1016/j.ijleo.2019.163903>.
- 4) Anis M, Baig MI, Alshehri AM, Somaily HH. Experimental analysis of pure and l-tyrosine influenced bis-thiourea zinc acetate (BTZA) crystal for NLO device applications. *Optik*. 2020;220:165100–165100. Available from: <https://doi.org/10.1016/j.ijleo.2020.165100>.
- 5) Azhar SM, Anis M, Rabbani G, Shirsat MD, Baig MI, Hussaini SS, et al. Growth of NH₄H₂PO₄ crystal in urea environment to optimize linear-nonlinear optical traits for photonic device applications. *Optik*. 2019;185:1247–1252. Available from: <https://doi.org/10.1016/j.ijleo.2019.03.041>.
- 6) Adhikari S, Kar T. Experimental and theoretical studies on physicochemical properties of l-leucine nitrate—a probable nonlinear optical material. *Journal of Crystal Growth*. 2012;356:4–9. Available from: <https://doi.org/10.1016/j.jcrysgro.2012.07.008>.
- 7) Najjar FA, Wakil GB, Want B. Electrical and mechanical studies on ferroelectric lithium rubidium sulphate crystals. *Journal of Advanced Dielectrics*. 2018;08(03):1850015–1850015. Available from: <https://doi.org/10.1142/s2010135x18500157>.

- 8) Aneeba B, Santhia SVA, Vinu S, Baazeem A, Christy RS. Effect of rare earth rubidium chloride on the optical, mechanical and antifungal behaviours of L-lysine monohydrochloride crystal for photonics and medical application. *Journal of King Saud University - Science*. 2021;33(5):101443–101443. Available from: <https://doi.org/10.1016/j.jksus.2021.101443>.
- 9) Khan SI, Kalainathan MI, Baig M, Shkir S, Alfaify HA, Ghramh. Mohd Anis, Linear-nonlinear optical, dielectric and surface microscopic investigation of KH_2PO_4 crystal to uncover the decisive impact of dopant glycine. *Mater Sci Poland*. 2018;36:662–667. Available from: <https://doi.org/10.2478/msp-2018-0073>.
- 10) Saravanakumar J, Chandrasekaran M, Krishnakumar B, Babu G, Vinitha M, Anis. Optimizing Optical Traits Of Ammonium Zinc Sulphate Hydrate Crystal Exploiting Nd^{3+} For Photonic Device Applications. *J Phys Chem Sol*. 2020;136:109133–109142. Available from: <https://doi.org/10.1016/j.jjleo.2019.163219>.
- 11) Baig MI, Anis M, Algarni HD, Shirsat MD, Hussaini SS. Customizing optical and dielectric traits of ammonium dihydrogen phosphate (ADP) crystal exploiting Zn^{2+} ion for photonic device applications. *Chinese Journal of Physics*. 2020;63:70–77. Available from: <https://doi.org/10.1016/j.cjph.2019.10.015>.
- 12) Tareev B. *Physics of Dielectric Materials*. 1979.
- 13) Kurtz SK, Perry TT. A powder technique for the evaluation of nonlinear optical materials. *IEEE Journal of Quantum Electronics*. 1968;4(5):333–333.
- 14) Park H, Kim TK, Cho SW, Jang HS, Lee SI, Choi SYY. Large-scale synthesis of uniform hexagonal boron nitride films by plasma-enhanced atomic layer deposition. *Scientific Reports*. 2017;7(1). Available from: <https://doi.org/10.1038/srep40091>.
- 15) Hanumantharao R, Bhagavannarayana G, Kalainathan S. Synthesis, growth, structural, optical, spectral, thermal and mechanical studies of 4-methoxy 4-nitrostilbene (MONS): A new organic nonlinear optical single crystal. *Spectrochim Acta A*. 2012;91:345–351. Available from: <https://doi.org/10.1016/j.saa.2012.07.128>.
- 16) Raj KR, Murugakoothan P. Effect of Co^{2+} on the growth and physical properties of potential nonlinear optical l-Asparaginium picrate crystal. *Optik - International Journal for Light and Electron Optics*. 2013;124(17):2696–2700. Available from: <https://doi.org/10.1016/j.ijleo.2012.08.032>.